Research Article | Vol. 24, No. 26 | 26 Dec 2016 | OPTICS EXPRESS 30164

Optics EXPRESS

Asymmetric diffraction from two-component optical gratings made of passive and lossy materials

GUANQUAN LIANG,[1] AYMAN ABOURADDY,[2] DEMETRIOS CHRISTODOULIDES,[2] AND EDWIN L. THOMAS[1,*]

[1]*Department of Materials Science and NanoEngineering, Rice University, Houston, TX 77005, USA*
[2]*CREOL, College of Optics and Photonics, University of Central Florida, Orlando, FL 32816, USA*
[*]*elt@rice.edu*

Abstract: Diffraction with asymmetric enhancement and suppression, and alternating contrast for symmetric diffraction orders is demonstrated from planar two-component optical gratings made of passive/lossy materials. Simulations agree well with the experimental diffraction pattern of the fabricated sample. Our fabrication approach uses simple, standard planar micro/nano lithography employing one photoresist and one dye. No 3D profiling is needed. The phenomena is due to the left-right asymmetric material distribution in the periodic grating, which gives rise to non-reciprocal light coupling for diffraction to the positive and negative orders.

OCIS codes: (050.1950) Diffraction gratings; (300.1030) Absorption; (220.4000) Microstructure fabrication.

References and links

1. P. Lalanne, S. Astilean, P. Chavel, E. Cambril, and H. Launois, "Design and fabrication of blazed binary diffractive elements with sampling periods smaller than the structural cutoff," J. Opt. Soc. Am. A **16**(5), 1143–1156 (1999).
2. Z. Lin, H. Ramezani, T. Eichelkraut, T. Kottos, H. Cao, and D. N. Christodoulides, "Unidirectional invisibility induced by PT-symmetric periodic structures," Phys. Rev. Lett. **106**(21), 213901 (2011).
3. L. Feng, Y. L. Xu, W. S. Fegadolli, M. H. Lu, J. E. B. Oliveira, V. R. Almeida, Y. F. Chen, and A. Scherer, "Experimental demonstration of a unidirectional reflectionless parity-time metamaterial at optical frequencies," Nat. Mater. **12**(2), 108–113 (2012).
4. M. Kulishov and B. Kress, "Free space diffraction on active gratings with balanced phase and gain/loss modulations," Opt. Express **20**(28), 29319–29328 (2012).
5. M. Kulishov, H. F. Jones, and B. Kress, "Analysis of PT-symmetric volume gratings beyond the paraxial approximation," Opt. Express **23**(7), 9347–9362 (2015).
6. S. V. Suchkov, A. A. Sukhorukov, J. Huang, S. V. Dmitriev, C. Lee, and Y. S. Kivshar, "Nonlinear switching and solitons in PT-symmetric photonic systems," Laser Photonics Rev. **10**(2), 177–213 (2016).
7. C. E. Rüter, K. G. Makris, R. El Ganainy, D. N. Christodoulides, M. Segev, and D. Kip, "Observation of parity-time symmetry in optics," Nat. Phys. **6**(3), 192–195 (2010).
8. A. Guo, G. J. Salamo, D. Duchesne, R. Morandotti, M. Volatier-Ravat, V. Aimez, G. A. Siviloglou, and D. N. Christodoulides, "Observation of PT-symmetry breaking in complex optical potentials," Phys. Rev. Lett. **103**(9), 093902 (2009).
9. L. Feng, X. Zhu, S. Yang, H. Zhu, P. Zhang, X. Yin, Y. Wang, and X. Zhang, "Demonstration of a large-scale optical exceptional point structure," Opt. Express **22**(2), 1760–1767 (2014).
10. Y. Yan and N. C. Giebink, "Passive PT Symmetry in Organic Composite Films via Complex Refractive Index Modulation," Adv. Opt. Mater. **2**(5), 423–427 (2014).
11. M. Botey, R. Herrero, M. Turduev, D. Zhao, I. Giden, H. Kurt, and K. Staliunas, "Asymmetric transmission from a 2D PT-symmetric honeycomb nanostructure," 2014 16th International Conference on Transparent Optical Networks (ICTON) We D5.4, http://ieeexplore.ieee.org/document/6876621/citations.
12. R. Birabassov, A. Yesayan, and T. V. Galstyan, "Nonreciprocal diffraction by spatial modulation of absorption and refraction," Opt. Lett. **24**(23), 1669–1671 (1999).
13. J. Albero, J. A. Davis, D. M. Cottrell, C. E. Granger, K. R. McCormick, and I. Moreno, "Generalized diffractive optical elements with asymmetric harmonic response and phase control," Appl. Opt. **52**(15), 3637–3644 (2013).
14. "Microchem SU-8 2000 series data sheet," http://www.microchem.com.
15. COMSOL Multiphysics software, *https://www.comsol.com/comsol-multiphysics*.

#275715 http://dx.doi.org/10.1364/OE.24.030164
Journal © 2016 Received 12 Sep 2016; revised 27 Nov 2016; accepted 27 Nov 2016; published 21 Dec 2016

Optics EXPRESS

16. W. M. Zhu, A. Q. Liu, X. M. Zhang, D. P. Tsai, T. Bourouina, J. H. Teng, X. H. Zhang, H. C. Guo, H. Tanoto, T. Mei, G. Q. Lo, and D. L. Kwong, "Switchable magnetic metamaterials using micromachining processes," Adv. Mater. **23**(15), 1792–1796 (2011).

1. Introduction

Asymmetric diffraction has been traditionally achieved by using a blazed optical grating that requires a complicated surface relief [1]. Recently, based on Parity-Time (PT) symmetry photonic systems [2,3], it was theoretically shown that it is possible to direct all the diffracted light to positive or negative orders by a grating with PT symmetry [4,5]. Such a PT symmetric grating requires that the refractive index modulation has a sinusoidal distribution for both the real and imaginary parts and a quarter periodicity spatial phase shift between them, which is a great fabrication challenge in practice. Balancing of gain and loss is another significant fabrication challenge, because a high value of gain is always difficult to obtain and in order to realize gain in the structure, a pumping mechanism has to be designed. In the literature, it has shown that via gauge transformations [6], practical PT symmetry can be generalized to include structures without balanced gain and loss [7], and even with pure loss [8]. Passive PT symmetry structures have also been demonstrated [9,10]. Reference [11] gives a simulation for dielectric cylinders on a 2D PT symmetric honeycomb lattice and shows asymmetric diffraction for the case that the wavelength is close to periodicity. Another way to generate asymmetric diffraction without providing surface relief, is to dope a polymer with two kinds of dyes at different bleaching wavelengths in order to obtain a special phase shift of the refractive index and absorption [12]. The experiment requires two dyes matching the available lasers. Another interesting example is to impart complicated periodic phase modulation into a spatial light modulator to asymmetrically split the incident beam to just one, two, three or four targeted orders [13]. However, a phase modulator is a device that needs complex electrical controls and is not easily integrated. It would be better to simplify the material choice and employ a standard lithography process to achieve a thin planar structure that provides asymmetric diffraction.

Here we demonstrate asymmetric diffraction from a simple planar two-component optical grating. The general scheme of the structure is shown in Fig. 1. By "two-component" we mean that two subsets of gratings compose the overall grating. Our structure corresponds to a compound one-dimensional grating with each period containing a pair of parallel grating lines belonging to the two sub gratings. The two subsets share the same thickness l and they have the same line widths ($a_1 = a_2$) but are made from different materials—one passive and the other one optically lossy. d_1 is the gap width between a_1 and a_2, with the period $p = a_1 + a_2 + d_1 + d_2$.

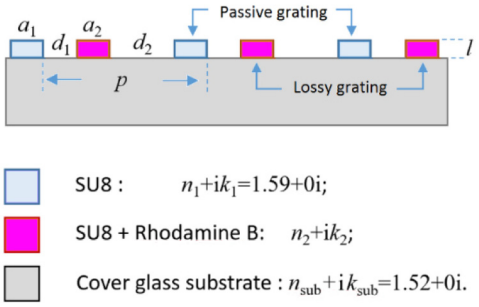

Fig. 1. Scheme for the two-component grating composed of two sub gratings having the same line widths ($a_1 = a_2$) but composed of a passive and a lossy material. The width between the two subgratings is denoted d_1.

Optics EXPRESS

2. Material preparation

Since we employ visible light at a wavelength of 532nm for our diffraction testing and the grating will be fabricated by UV photo lithography, SU-8 was chosen for the passive material which is readily photo-crosslinkable through UV exposure and has almost no absorption in the visible [14].

To create the lossy material, we doped SU-8 with the dye Rhodamine B (RhB) at various weight percentages (wt%) to generate optical lossy material (SU-8:RhB). In our fabrication, the lossy grating is formed by patterning a cured SU-8:RhB film, hence it is necessary to obtain the real and imaginary part of refractive index of this film material for numerical simulation of diffraction and for comparison to experimental results. For this purpose, we measured the transmission (T) of the film, from which the absorption coefficient (α) at particular wavelength λ_p can be calculated from Lambert's law:

$$\alpha(\lambda_p) = -\log_{10}[T(\lambda_p)]/l \tag{1}$$

where $T(\lambda_p)$ is the transmission that can be measured by UV-VIS-NIR Spectroscopy, and l is the film thickness. From our calculated discrete values of absorption coefficients as a function of wavelength, we use the Kramers-Kronig (K-K) relation to evaluate the corresponding change in the real part of refractive index Δn for a given wavelength λ:

$$\Delta n(\lambda) = \frac{1}{2\pi}\sum_{p=1}^{q}\frac{\alpha(\lambda_p)}{1-(\lambda_p/\lambda)^2}\Delta\lambda_p \tag{2}$$

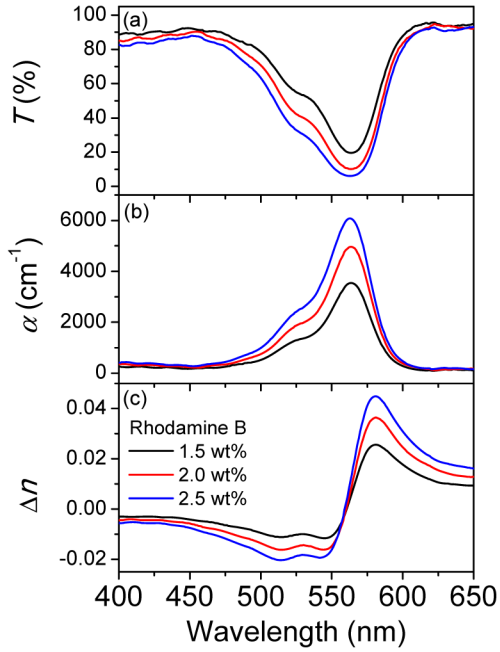

Fig. 2. (a)Transmission, (b) Absorption coefficient, and (c) Change in the real part of refractive index for cured SU-8:RhB films doped with different wt% Rhodamine B according to the different line color: black 1.5wt%, red 2.0wt%, and blue 2.5wt%.

To prepare the SU-8:RhB films, we used SU-8 2002 with 29wt% SU-8 dissolved in cyclopentanone. Figure 2(a) shows transmission of SU-8:RhB films as a function of the wt% of RhB, measured by UV-VIS-NIR Spectroscopy (SHIMADZU). The film thickness is about 2um, and according to Lambert's law, the calculated absorption coefficients (α) are shown in

Optics EXPRESS

Fig. 2(b). Figure 2(c) shows the corresponding change in the real part of the refractive index Δn. At 532nm, with 1.5, 2.0, and 2.5 wt% RhB doping, α = 3230, 4708, and 6172 cm^{-1}, respectively; and the corresponding values of imaginary part of refractive index ($k = \alpha\lambda/4\pi$) are 0.0137, 0.0199, and 0.0261, respectively; and thus Δn = –0.010, –0.014, and –0.018, respectively. Since at this wavelength the refractive index of SU-8 is 1.59 + 0i, as an example, for SU-8:RhB with 2.5 wt% RhB doping, the refractive index becomes 1.572 + 0.0261i.

3. Simulation

We next simulate the transmission diffraction of a two-component grating by a far field calculation using the Electromagnetic Waves Frequency Domain module in COMSOL Multiphysics [15]. The structural parameters employed are p = 25um, $a_1 = a_2$ = 5um, l = 0.95um. We use normal incidence for all the simulations below.

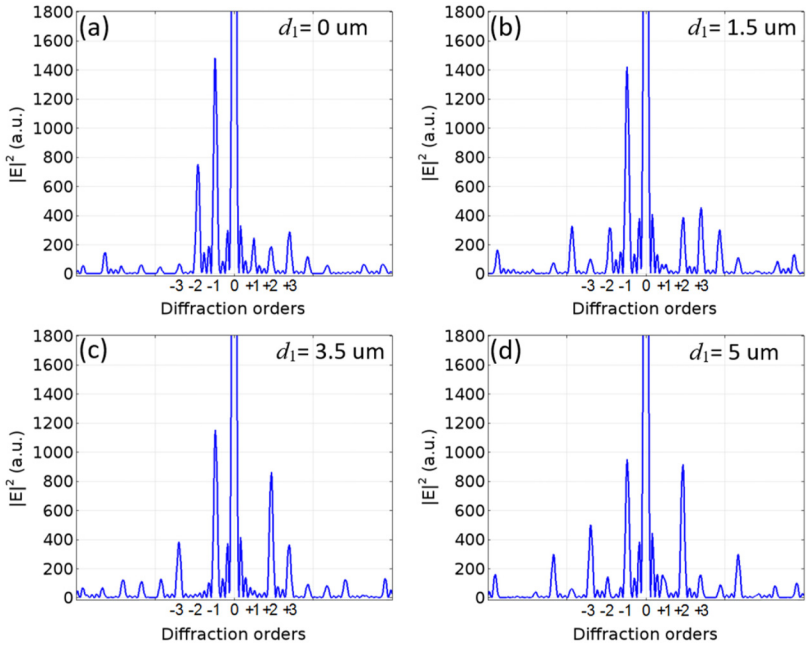

Fig. 3. Effect of gap width d_1 on simulated diffraction of two-component (passive 1.59/lossy 1.572 + 0.0261i) gratings with periodicity 25um, grating line widths $a_1 = a_2$ = 5um, thickness l = 0.95um, and different gap widths d_1: (a) 0 um, (b) 1.5um, (c) 3.5um, and (d) 5um.

Figure 3 shows typical results of a series of gratings varying the gap width d_1. When d_1 = 0, as shown in Fig. 3(a), we have very strong diffraction to the −1st and −2nd orders with intensities much higher than the + 1st and + 2nd orders and indeed all the others. This is a close result to the PT symmetric grating having sinusoidal modulation as in references [4] and [5]. When the gap width increases to 1.5um, as shown in Fig. 3(b), only the −1st order of diffraction is enhanced while the + 1st order is completely suppressed, with low diffraction intensity for all other orders. When the gap width further increases to 3.5um, as shown in Fig. 3(c), we have not only the −1st order enhanced and + 1st order completely suppressed, but also the + 2nd order enhanced and −2nd order completely suppressed. Diffraction into the +/−1st orders and the +/−2nd orders displays alternate changes in contrast. When the gap width reaches 5um, as shown in Fig. 3(d), the −1st and + 2nd orders are still enhanced and in addition, the −3rd order is enhanced, although the + 1st, −2nd and + 3rd orders are not completely suppressed. Note that the alternate change in contrast extends to the +/−3rd order.

Optics EXPRESS

Further increasing the gap width d_1 to the limit of 7.5um (because p = 25um and $a_1 = a_2$ = 5um) results in less and less asymmetric enhancement and suppression.

In order to see the impact of different kinds of refractive index combinations on the diffraction, we compare the situation of balanced index difference in the real and imaginary parts, to situations like asymmetric-real and symmetric-imaginary potentials; or symmetric-real and asymmetric-imaginary potentials. Figure 4 is for a sublattice gap width d_1 = 1.5um, with four panels showing four different combinations of refractive indexes. In Fig. 4(a) we use a combination of passive and lossy materials with refractive indices corresponding to 1.59 + 0i and 1.56 + 0.03i, having a balanced difference in the real and imaginary parts, giving similar results as that in Fig. 3(b) where the indices are not well balanced. In Fig. 4(b), we use a combination of passive and lossy materials with refractive index 1.59 + 0i and 1.59 + 0.03i, which has symmetric real and asymmetric imaginary potentials. In Fig. 4(c), we use a combination of lossy materials with refractive index 1.59 + 0.03i and 1.56 + 0.03i, which has asymmetric real and symmetric imaginary potentials. In Fig. 4(d) we use a combination of balanced gain and lossy materials with refractive indices of 1.59-0.015i and 1.56 + 0.015i.

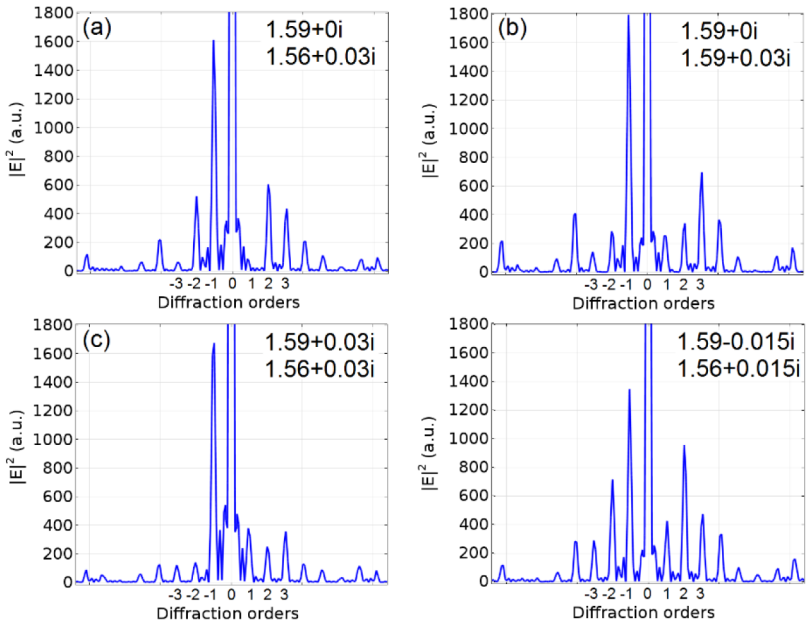

Fig. 4. Effect of different refractive index combinations (as marked in the panels) on simulated diffraction of two-component gratings with periodicity 25um, grating line widths $a_1 = a_2$ = 5um, thickness l = 0.95um, and gap width d_1 = 1.5um. (a) Balanced difference in real and imaginary refractive index (passive and lossy materials); (b) Symmetric real and asymmetric imaginary index (passive and lossy materials); (c) Asymmetric real and symmetric imaginary index (lossy materials); and (d) Balanced difference in real and imaginary refractive index (gain and lossy materials).

Figure 4 shows that for the structural parameters used, all four material combinations give asymmetric diffraction patterns. However, the precisely balanced gain and loss combination in Fig. 4(d) does not give the most asymmetric diffraction for the +/– 1st orders, as compared to that in Fig. 4(a). For practical fabrication, a high gain value is difficult to obtain. Comparing the material combinations in Fig. 4(a)(b) and (c), the combination of a passive with a lossy material is the easiest way to go because it requires only one kind of photoresist and one kind of doping. Via the Kramers-Kronig relation, variation of the imaginary part of the refractive index must at the same time, change the real part. For most choices of materials, an imbalance between the real and imaginary parts results, which still gives asymmetric

Optics EXPRESS

diffraction, as shown in Fig. 3. However, in order to realize the combinations of symmetric real or imaginary part of refractive index, like those in Fig. 4(b) or (c), we need to have at least two kinds of photoresists, and this may introduce complications or incompatibility for fabrication.

Qualitatively, the phenomena are due to the left-right asymmetric material distribution of the periodic grating, which gives rise to non-reciprocal light coupling for diffraction to the positive and negative orders. In our results, one interesting phenomenon is that the first order diffraction is always asymmetric and not affected much at all with changes in the width of d_1; while the higher order diffraction orders are influenced by the width of d_1. This is expected since the first order diffraction is mainly influenced by the periodicity, while higher order reflections depend on the finer scale structural detail. From another point of view, a smaller d1 gives more asymmetric diffraction because it makes each pair of the passive/lossy grating lines closer to the optical effects of a triangular surface relief of a blazed grating. The passive line of the two-component grating corresponds to the thicker part of the triangular relief because of its higher real part of refractive index which corresponds to a longer optical path; while the lossy line corresponds to the thinner part of the triangular relief because of its lowered real part of refractive index due to the RhB doping. Note that our planar "blazed grating" gives transmissive asymmetric diffraction, not the reflective diffraction of a traditional blazed grating. The above results are also somewhat sensitive to the thickness of the grating. The diffraction of incident 532 nm wavelength at other grating thicknesses is less interesting unless the thickness reaches approximately an integral multiple of the thickness (0.95 um), which means such asymmetric diffraction results from the interference of the scattered light whose intensity and phase are affected by the lossy material and the thickness of the grating.

4. Fabrication, characterization and discussion

The fabrication process for the two-component grating with passive and lossy materials is schematically shown in Fig. 5. We fabricate the passive grating first [Fig. 5(a)-(e)]. A triple layer thin film stack S1818/LOR/SU-8(cured) on cover glass is prepared as shown in Fig. 5(a) before the UV patterning exposure (Mask Aligner EVG 620) is made through a chrome photomask. The photomask has only one grating pattern which defines one grating line width and the overall periodicity. S1818 (from Shipley) is an UV sensitive positive tone photoresist, and LOR (from Microchem) is the lift-off resist used for making the undercut profile. S1818 is developed in solvent MF-319 and the immersion of the LOR in solvent MF-319 [Fig. 5(b)] gives the undercut profile for later sputter coating of Au [Fig. 5(c)] and the subsequent lift-off process [Fig. 5(d)] to produce a first Au grating on top of the cured SU-8 layer. To obtain a stable undercut, the thickness of the LOR layer is made smaller than the grating line width by further diluting the solution of LOR 30B. Then an RIE process (Oxford Plasmalab System 100), with O_2 gas 3 sccm, pressure 1mTorr, RIE power150W, and substrate temperature 10°C) is applied to vertically etch down the cured SU-8 layer to obtain the passive SU8 grating under the Au cap protection [Fig. 5(e)]. The etching rate was measured to be about 1 nm/s.

Immediately after the above passive grating fabrication processes, we next fabricate the lossy grating [Fig. 5(f)-(j)]. As shown in Fig. 5(f), SU-8:RhB is spin coated to bury the passive grating, then is cured using flood UV exposure and post exposure bake as for the pure SU-8, but a longer bake time is needed to account for the doping level of RhB. We find that the maximum curable doping level is between 2.5 to 3 wt%. We need to fully cure the SU-8:RhB layer to avoid strong swelling or dissolution by the cyclopentanone in the LOR solution. We then image the cross section with SEM to obtain the thicknesses of the passive SU-8 grating and the cured SU-8:RhB layer, and accordingly RIE (same recipe as before) is applied to thin the SU-8:RhB layer to be the same thickness as the passive SU8 grating, so that we will have the same thickness for the two sets of gratings. After this, the LOR and

Optics EXPRESS

S1818 layers are formed by spin coating on top of the hybrid layer which contains the passive SU-8 grating with the Au protection cap with the SU-8:RhB material in between the SU8 regions. Then a shifted UV exposure is performed on top of SU-8:RhB by a second photomask, which has a designed lateral shift to the first photomask used for the passive grating, as shown in Fig. 5(g). After repeating the same processes of development, sputtering Au, and lift-off as in Fig. 5(b)-(d), two sets of Au caps are formed on top as the protection of underneath layer [Fig. 5(h)]. The next step is RIE which etches down through the SU-8:RhB material [Fig. 5(i)]. Finally after Au etchant immersion and deionized water rinse, the two-component grating is achieved with one passive subgrating and the other lossy subgrating, as shown in Fig. 5(j) and Fig. 6(a).

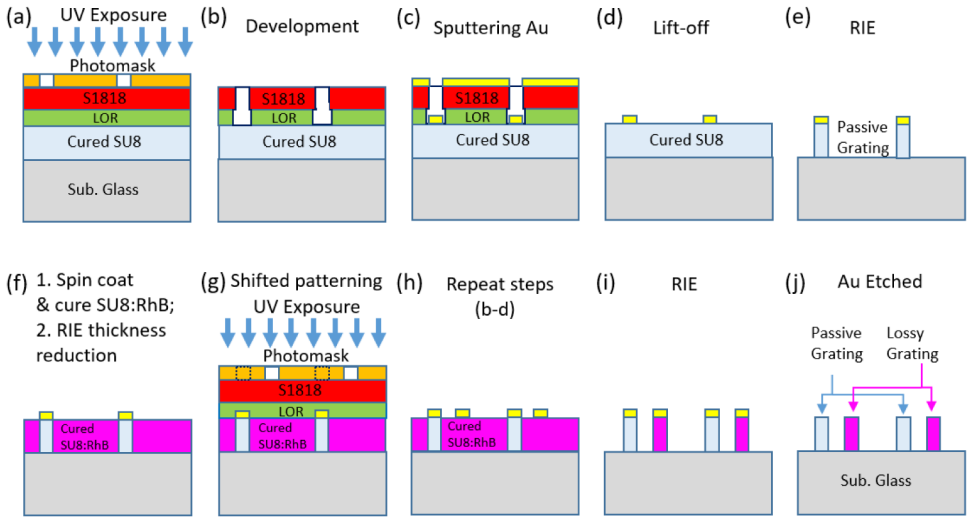

Fig. 5. Scheme of the fabrication work flow for two-component passive/lossy optical gratings.

An optical image of the two-component passive/lossy grating is shown in Fig. 6(a). Periodically arranged pairs of parallel lines are obtained on the cover glass substrate, with the bright set being made of SU-8 and the pink-red set made of SU-8:RhB (2.5wt%). Figure 6(b) is a SEM secondary electron image viewing normal to the film surface and Fig. 6(c) is the SEM cross sectional image. The periodicity is 25 um as defined by the photomask; the grating line width is about 6.10 um for the passive set and 6.35 um for the lossy set; the width of the small gap between them is about 1.30 um; and the layer thickness is approximately 0.95 um.

We next perform diffraction on the passive/lossy grating using normal incident 532 nm cw laser light (Coherent, Verdi 5). The diameter of the incident beam is about 1 mm defined by a circular aperture and the power is set at about 2 mW. An optical image of the diffraction pattern is shown in Fig. 6(d), which reveals the strongly asymmetric diffracting ability of the fabricated grating as can be seen by examination of the diffraction intensity distribution for the +/– 1st and +/– 2nd orders. The diffraction intensity of each order can be quantified using a laser power meter, as shown in Fig. 6(e), and the difference between +/– 1st orders is about 7.5 times, with the –1st order much stronger than all the others. Alternate contrast occurs for +/–1st and +/– 2nd orders. The inset of Fig. 6(e) shows the diffraction simulation employing the experimentally measured grating dimensions and the real and imaginary refractive index values calculated before. The agreement between experiment and simulation is quite good.

Optics EXPRESS

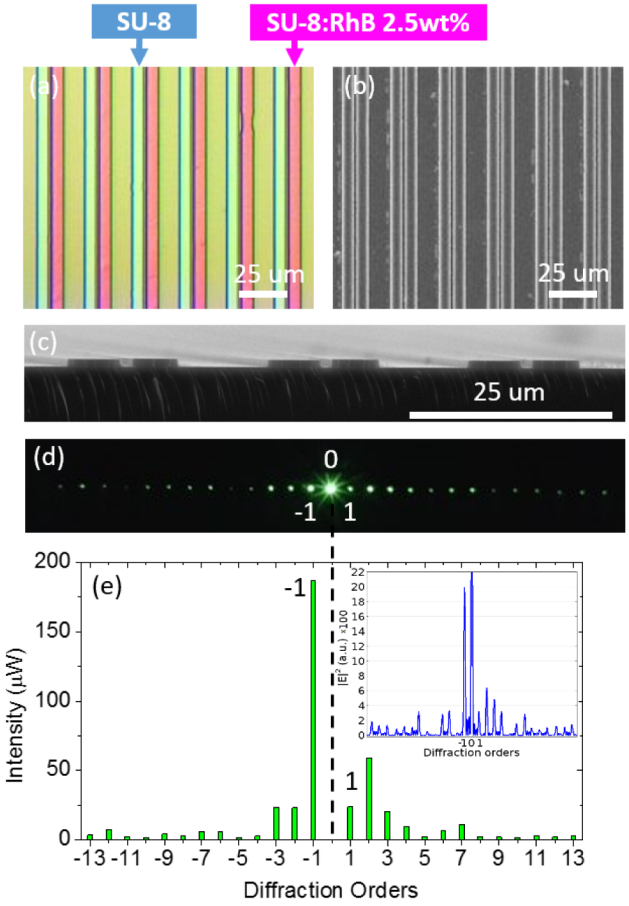

Fig. 6. (a) Optical microscope image; (b) top view and (c) cross section SEM Images of the fabricated two-component grating with one set made of passive SU-8 and one set of lossy SU-8:RhB; (d) 532 nm laser diffraction test; (e) Measured intensities of the diffraction orders in (d). Inset: simulation. The negative order side has the −1st order diffraction much stronger than all the other orders. Alternate contrast occurs for +/−1st and +/− 2nd orders.

For future experiments that demonstrate results from simulations, we need to address the fabrication accuracy. By current fabrication scheme, to pattern the two sub sets of gratings made of different materials, it involves two separate sets of exposure and development processes. The thickness of the spin coated S1818 layer prepared for each exposure may vary, and it will give different patterning line widths at the interface between S1818 and LOR, because UV light intensity will be different when it reaches the interface through different thicknesses of S1818. On the other hand, development of a photoresist is a wet chemical process which is not easy to precisely control. The fabrication scheme can be improved to pattern two different materials for the two sub sets of gratings at the same time, so that better control of line widths for them will be achieved. First, use a photomask defining a set of passive grating with wider line width than as needed, and the work flow can follow Fig. 5(a)-(e). Immediately after this, selectively etch away the Au protection for the passive grating, but keep those Au protection on the markers made by the first exposure for alignment in the second exposure. Then spin coat lossy material to bury the passive grating and use RIE to thin them to the same thickness. After this, a photomask that defines two sub sets of gratings with narrower line widths can be aligned. This can be guaranteed by well-designed alignment markers to align the second patterning to the first patterning. By this way, the line width for

Optics EXPRESS

each set of grating on different materials will be well defined and can be made the same or different as needed.

5. Conclusion

In conclusion, we have explored diffraction from two-component polymeric optical gratings made of passive/lossy materials. We found not only strong asymmetric diffraction to one side of the diffraction orders which is comparable to that by a PT symmetric diffraction grating with sinusoidal refractive index modulation; additionally other interesting phenomena are shown, such as alternate diffraction contrast can happen for the +/– 1st, 2nd and 3rd orders by the adjustment of the gap width between the two-component grating. A fabrication scheme was proposed and realized to demonstrate asymmetric diffraction; and the experiment is in good agreement with simulation. Concerning the fabrication accuracy of grating line widths, an improved fabrication scheme is also proposed for future fabrication. For a future study, it will be interesting to extend the asymmetric enhancement and suppression of certain diffraction orders to higher ones and to achieve alternative diffraction contrast to higher orders beyond the +/– 3rd orders by more comprehensive structural design and material choice. It may be enough to use one kind or even two kinds of passive/lossy materials and simple two-component geometry design; but extending the choice of materials to gain materials and the geometry to three or four geometry components, will definitely increase the possibility in discovering new kinds of coding for diffraction patterns. Applications of our diffraction control can be in signal coding and processing where simultaneous multichannel control of optical information is desired. To make our device switchable, all is need is to fabricate each sub grating separately on a glass substrate, then assemble them face-to-face to make the two sets become a two-component grating. By fixing one substrate and using a piezo stage to move the other grating with respect to the first, the gap d_1 between the two subsets of gratings can be tuned, so that dynamic coding can be realized. This idea would be similar to the switchable mechanism in MEMS [16].

Funding

AFOSR (Air Force Office of Scientific Research, U.S.A.) MURI (DoD Multidisciplinary University Research Initiative: FA9550-14-1-0037.